# Post-Print

# A Preliminary Kinetic Characterization of LiAlH$_4$ and Li$_3$AlH$_6$ for Airbreathing Propulsion

Matteo Boiocchi[*], Luciano Galfetti[†], Luca Di Landro[‡]
*Politecnico di Milano, Milan, Italy, 20156*

**The aim of this research is to present a preliminary experimental investigation on the use of lithium-aluminum complex hydrides in the field of airbreathing propulsion. It is known that a launch system based on the airbreathing technology, by using air as oxidizer, reduces the cost per kg of the launch, and is therefore much more profitable than common rocket engines (solid and liquid rockets). The effect of nitrogen gas on the thermal behavior and the kinetic parameters of lithium aluminum hydride (LAH, LiAlH$_4$) and tri-lithium aluminum hydride (L3AH, Li$_3$AlH$_6$) has been investigated. DSC tests, performed using nitrogen gas, have shown the presence of a strong exothermic peak which, when using helium or argon gas, is barely noticeable. A nitridation reaction has been suggested to explain the increase of the sample mass after each DSC test, which supports the experimental data. The activation energy E$_a$ and frequency factor A for the samples of LAH and L3AH have been calculated using two simplified kinetic methods: Ozawa method and Kissinger method.**

## Nomenclature

A = Pre-exponential factor, min$^{-1}$

DSC = Differential Scanning Calorimeter

E$_a$ = Activation energy, KJ/mol

k(T) = Rate constant, min$^{-1}$

L3AH = Trilithium Aluminum Hexahydride, Li$_3$AlH$_6$

LAH = Lithium Aluminum Hydride, LiAlH$_4$

---

[*] Ph.D., Department of Aerospace Science and Technology, via La Masa 34.
[†] Full Professor, Department of Aerospace Science and Technology, via La Masa 34.
[‡] Associate Professor, Department of Aerospace Science and Technology, via La Masa 34.

| $M_{fin}$ | = | Final sample mass, mg |
|---|---|---|
| $M_{in}$ | = | Initial sample mass, mg |
| R | = | Perfect gas law constant, KJ/mol K |
| $T_p$ | = | Peak temperature, °C |
| α | = | Extent of reaction, % |
| β | = | DSC heating rate, K/min |
| Δh | = | Heat of reaction, J/g |
| ΔM | = | Percentage mass variation, % |

## I. Introduction

FOR many years, several studies focusing on the employment of hydrogen for advanced technological applications have been carried out. The use of hydrogen containing substances as energetic materials is the main topic of most of such investigations. The implementation of a hydrogen-based energy economy conceals great challenges, especially regarding the identification and characterization of a proper effective and safe hydrogen storage medium. Material-based approaches to hydrogen storage using hydrides and amides are being deeply studied. Research activities on metal hydrides used as energetic fillers in solid fuels for hybrid rocket propulsion have been carried out since 1966 [1]. The combustion of metal powders is highly exothermic and moreover, the presence of hydrogen leads to significant performance improvements and many energetic and propulsive benefits [2-6]; enhancement of the energetic content of the fuel, increase of the specific impulse and regression rate, increased easiness to ignite the fuel are few examples of the attained improvement. Linked to the needs of reducing the cost per kg of the common rocket launchers it was estimated that by replacing the second stage of a three-stage rocket system with a scramjet motor, the overall payload mass can be increased roughly by 50%, decreasing strongly the cost per launch [7-8]. The implementation of an effective and affordable scramjet rocket system conceals great challenges especially linked with the difficulties to study combustion phenomena at supersonic conditions both from an experimental and numerical point of view [9-10]. Dimotakis [11] studied various launch options for launching small payloads to Low Earth Orbit (LEO). He considered various launch systems such as: single- and multi-stage, ground- and air-launched rockets in order to demonstrate the advantages implied when an intermediate airbreathing boost stage is used. The pioneering investigation on solid fueled scramjet was performed for the first time by Witt [12], using PMMA and HTPB as solid fuels. He evidenced that a small cavity internal to the combustion chamber improves

ignition and sustainability of combustion. Angus [13], continuing Witt's work, discovered that by using a small amount of hydrogen gas, the ignition process is facilitated and also the sustainability of the flame strongly increases. The effect of PMMA and HTPB filled with metal powders as energetic additive, on the self-ignition and self-sustained combustion in solid-fueled scramjet engines, was proved by Cohen and Natan [14]. Early studies carried out by Simone and Bruno [15] showed theoretically the advantages to use LiH as bifuel for solid-fueled-scramjet; the benefits are linked both with the high energy density usual for metal hydrides, and with the safety of such hydrogen carrier. In 1991, Rhein [16] studied the ignition and combustion behavior of lithium under different physical conditions; the influence of nitrogen gas and moisture in air on the combustion of lithium was especially analyzed. The aim of such preliminary work was to investigate the possibility to use metallic lithium as fuel for ramjet/scramjet military applications. The present work is intended to study the decomposition mechanisms of lithium aluminum hydride and trilithium aluminum hydride in presence of nitrogen gas.

Early studies by Dymova [17], Andreasen [18] and Ismail [19] described the decomposition process considering five stages involving different reactions and thermal effects, which may partially overlap: the first exothermic peak has been assigned to the interaction of LAH with surface hydroxyl impurities; equation 1 shows the reaction of surface aluminum hydroxyl with Al hydride, producing hydrogen [20].

$$Al - OH + H - Al \rightarrow Al - O - Al + H_2 (g) \qquad (1)$$
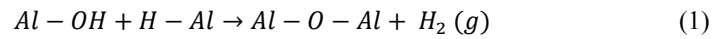
The first endothermic peak corresponds to the melting of LAH:

$$LiAlH_4 (s) \rightarrow LiAlH_4 (l) \qquad (2)$$

The melting of the LAH is immediately followed by a second exothermic peak corresponding to the decomposition of liquid LAH:

$$LiAlH_4 (l) \rightarrow 1/3 \ Li_3 AlH_6 (s) + 2/3 \ Al (s) + H_2 (g) \qquad (3)$$
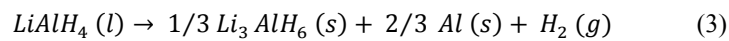
The second endothermic peak corresponds to the decomposition of $Li_3AlH_6$ as described by [21]:

$$1/3 \ Li_3AlH_6 (s) \rightarrow LiH (s) + 1/3 \ Al (s) + 1/2 \ H_2 (g) \qquad (4)$$
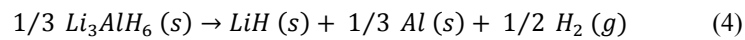
The last step of decomposition has been assigned to the decomposition of lithium hydride:

$$LiH (s) \rightarrow Li + 1/2 \ H_2 \ (g) \qquad (5)$$
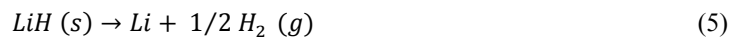
As stated by Block [20], at high contamination levels, the observed heat deviates from that found for low levels, because of increasing complexity and/or incompleteness of the reaction.

## II.Thermal analysis: kinetic calculations

Several numerical methods [22] have been proposed to obtain the most important kinetic parameters by starting from TGA or DSC thermographs performed at different heating rates even when the reaction order is not known. "Model-free" kinetics is often adequate to describe the kinetics of complex reactions either of organic and inorganic compounds. The most used "model free" methods can be summarized as: Friedman method [23], Kissinger method [24], Flynn-Wall-Ozawa method [25] and Doyle method [26]. In order to determine the kinetic parameters of the decomposition reactions of pure LAH and L3AH, Ozawa and Kissinger's methods were applied. They were both derived from the basic kinetic equations for heterogeneous chemical reactions and therefore have a wide application, as it is not necessary to know the reaction order or the conversional function to determine the kinetic parameters. The activation energy determined by applying these methods is the sum of activation energies of chemical reactions and physical processes occurring in thermal decomposition and therefore it is called apparent activation energy. However it assumes a specific value referring to a single reaction step [27]. The temperatures of exothermic peaks, $T_p$, can be used to calculate the kinetic parameters both by Ozawa method and Kissinger method (activation energy $E_a$, and pre-exponential factor A of the decomposition process). The $E_a$ value is the minimum energy required to initiate the decomposition reaction, while the A value is related to the frequency of interaction among the atoms. The $E_a$ and A values are indispensable for decomposition kinetics, based on the Arrhenius equation:

$$k = A * e^{-E_a/_{RT}} \qquad (6)$$

where k is the rate constant, T is the temperature and R is the perfect gas law constant. By introducing the conversion degree α (the extent of the chemical reaction), the previous equation can be expressed as follows:

$$d\alpha/dt = f(\alpha)Ae^{-E_a/_{RT}} \qquad (7)$$

Where t is the reaction time and f(α) is the kinetic model function in differential form. In DSC tests, the conversion degree α can be easily calculated by the ratio between the enthalpy at the time t and the total heat of reaction.

By integrating the previous equation, it can be obtained:

$$g(\alpha) = \left(^{AE_a}/_{R\beta}\right)p(x) \qquad (8)$$

with $g(\alpha) = \int_0^\alpha d\alpha/f(\alpha)$ and $p(x) = \int_x^\infty \frac{e^{-x}}{x^2} dx$ where $x = ^{E_a}/_{RT}$

In the Kissinger method, the conversion degree α = const at the top of the DSC peak, by using the Kissinger's approximation, equation 7 can be written as:

$$-ln\left(\beta/T_p^2\right) = E_a/RT_p - \ln\left(AR/E_a\right) + \ln g(\alpha_p) \qquad (9)$$

Where $\alpha_p$ represents the extent of the reaction reached at the top of the peak, where the temperature value is $T_p$. According to the Kissinger equation, the plot of $-\ln(\beta/T_p^2)$ versus $1000/T_p$ should be linear and the activation energy value is obtained from the slope of the line. Sbirrazzuoli [28] reported that the Kissinger-Akahira-Sunose method (KAS), which is an extension of the Kissinger method, is valid for $20 \leq E_a/RT \leq 50$.

In the Ozawa method, by assuming to use the temperature value at the top of the peak $T_p$ and by using Doyle's approximation, equation 7 can be written in a logarithmic form:

$$Log\ g(\alpha_p) = \log\left(AE_a/R\right) - \log \beta - 2.315 - 0.457\,E_a/RT_p \qquad (10)$$

Again, by fitting the plot obtained using $\log \beta$ versus $1000/T_p$ a straight line can be obtained and the slope $(-0.457E_a/R)$ indicate the needed activation energy value. As stated by Flynn [25], at the limits $20 \leq E_a/RT \leq 60$, the equation 10 is accurate within $\pm 3\%$.

Analyzing the accuracy of the used approximated methods in determining the activation energy, Farjas [29] showed that the relative error of KAS method is not relevant (<2%), on the contrary, the relative error of FWO (Flynn-Wall-Ozawa which is an extension of Ozawa method) method can be as high as 15%.

The activation energy and kinetic parameters of thermal decomposition of lithium-based samples were calculated both by Ozawa and Kissinger methods. Dynamic scans were conducted at heating rates of 10 to 50 K min$^{-1}$, and were used to determine the heat of reaction and kinetic parameters such as activation energy and the frequency factor. The method of least squares was applied to evaluate the estimated standard error of the slope of the regression lines obtained applying both Ozawa and Kissinger's methods. By knowing the standard error of the slope of the line and also a 95% confidence interval for the same parameter, by simple calculations, a range of $E_a$ values was obtained (Table 2, 4 and 5).

## III. Experimental Investigation

### A. Materials

The first investigated material was lithium aluminum hydride supplied by Chemetall Gmbh (LiAlH$_4$, LAH), with a purity of 95 - 97% by mass. The second was trilithium aluminum hexahydride (Li$_3$AlH$_6$, L3AH), which was supplied

by the same company. The purity value was 95 - 97% as indicated by Technical Data Sheet. The theoretical hydrogen content is respectively: 10.6% and 11.2%. Both the LAH and L3AH samples were filtered by using a sieve, in order to eliminate impurities similar to small stones with an average diameter between 0.5 mm to 5 mm. The larger fraction of the product was in the shape of powder with average diameter between 10 and 200 μm. All these operations were carried out in a glove box under nitrogen atmosphere.

**B. Thermal analysis: differential scanning calorimetry**

The experimental investigation was carried out using the differential scanning calorimetry (DSC) technique (TA instruments, model 2010 CE). This study was done using aluminum capsule pan, under a nitrogen flux (38 ml/min), at different heating rates, between 0 and 350 °C. Heating rate values spanning between 10 and 50 K/min were selected; the samples (2.2 - 2.4 mg) were placed in an uncovered aluminum pan to allow an intimate contact between the nitrogen gas and the sample. The weight of the samples was measured at different reaction stages.

## IV. Experimental Investigation

### IV.A. Kinetic Calculations: LAH

The DSC dehydrogenation curves of pure LAH as a function of the heating rate are shown in Figure 1. Two exothermic peaks and two endothermic peaks are evidenced in the thermographs; Table 1 shows the peak temperature of the different thermal events at different heating rate (10, 15, 20, 25, 30, 40 and 50 K/min). The first exothermic peak temperature occurs in a narrow range between 160 – 169 °C, depending on heating rate; it is followed by an endothermic peak in the range 167 – 170 °C, which overlaps to the previous exotherm and disappears when heating rates exceed 15 K/min. The second exothermic peak occurs in the temperature range 189 – 216 °C. The last endothermic peak is in the range 255 – 280 °C. An average increase in sample mass of $26.9 \pm 10\%$, at the end of DSC tests, was measured. On the basis of the obtained experimental trends and applying the Ozawa and Kissinger techniques, the activation energy $E_a$ and the frequency factor A were evaluated and discussed.
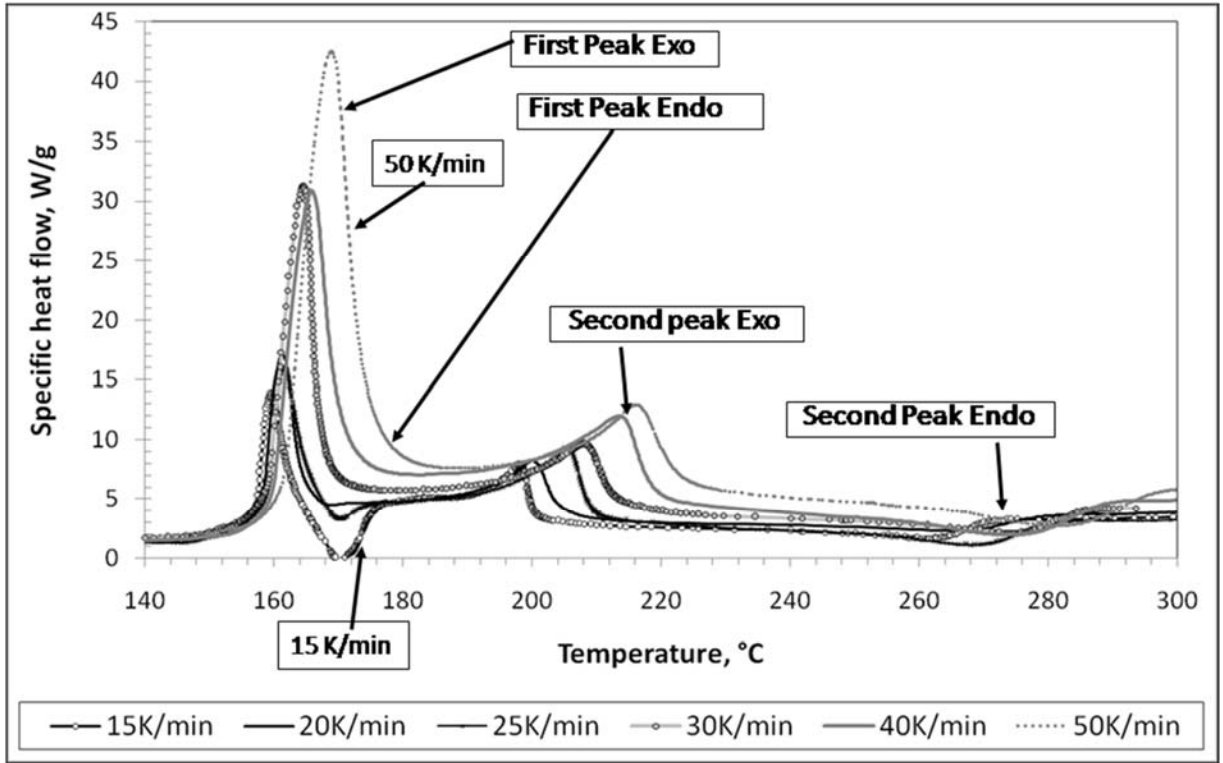
Figure 1. DSC thermographs obtained at different heating rate values: LAH.

**Table 1. List of temperature peak values with the corresponding initial and final sample mass for LAH**

| β [K/min] | 1st Exo $T_p$ [°C] | 2st Exo $T_p$ [°C] | 1st Endo $T_p$ [°C] | 2nd Endo $T_p$ [°C] | 1st+2nd Exo Δh (125-225°C) [J/g] | 2nd Endo Δh (225-325°C) [J/g] | $M_{in}$ ± 0.1mg [mg] | $M_{fin}$ ± 0.1mg [mg] | ΔM [%] |
|---|---|---|---|---|---|---|---|---|---|
| 10 | 162.0 | 188.8 | 167.3 | 254.5 | 843 | 123 | 2.2 | 2.9 | 31.8 ± 10.6 |
| 15 | 159.6 | 198.4 | 170.2 | 260.9 | 599 | 151 | 2.2 | 2.8 | 27.3 ± 10.8 |
| 20 | 161.4 | 200.2 | - | 265.2 | 636 | 115 | 2.3 | 2.9 | 26.1 ± 9.9 |
| 25 | 163.5 | 204.5 | - | 270.3 | 746 | 129 | 2.3 | 2.9 | 26.1 ± 9.9 |
| 30 | 164.7 | 208.1 | - | 274.5 | 668 | 122 | 2.3 | 2.9 | 26.1 ± 9.9 |
| 40 | 165.9 | 213.6 | - | 273.8 | 689 | 135 | 2.4 | 3.0 | 25.0 ± 9.4 |
| 50 | 168.9 | 216.1 | - | 281.6 | 656 | 109 | 2.3 | 2.9 | 26.1 ± 9.9 |
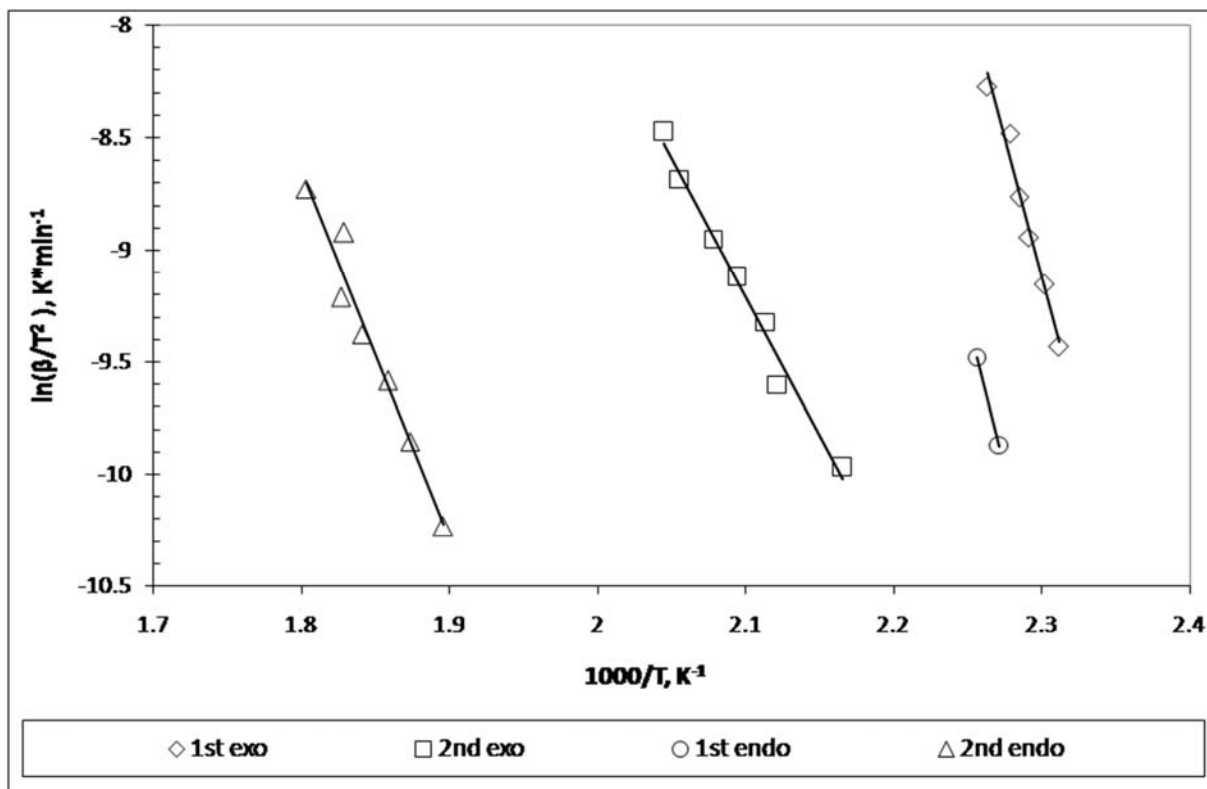
Figure 2. Kinetic DSC elaboration (plotting $-\ln(\beta\, T_p^2)$ vs. $1/T_p$ according to Kissinger's method): LAH.

Figure 2 shows the kinetic elaboration according to Kissinger's method by which, by plotting $\ln(\beta\, T_p^2)$ vs. $1/T_p$ the activation energy ($E_a$) and the pre-exponential factor (A) values, listed in Table 2, were calculated. Kissinger and Ozawa methods were applied by using the slope and the intercept of the regression lines (eq. 9 and eq. 10).

**Table 2. Kinetic parameters for LiAlH$_4$, calculated by both Kissinger and Ozawa method**

| Kinetic Parameter | Method | 1$^{st}$ Exo 162 – 169°C | 2$^{nd}$ Exo (189 – 216°C) | 2$^{nd}$ Endo (255 – 282°C) |
|---|---|---|---|---|
| $E_a$ [KJ/mol] | | 201.01±34.64 | 105.42±13.54 | 138.56±27.12 |
| A [min$^{-1}$] | Ozawa | $(3.75\pm0.24)*10^{24}$ | $(4.66\pm0.31)*10^{11}$ | $(3.17\pm0.34)*10^{13}$ |
| $R^2$ | | 0.98 | 0.99 | 0.97 |
| $E_a$ [KJ/mol] | | 204.13±36.34 | 102.84±14.20 | 136.73±28.54 |

| A [min$^{-1}$] | Kissinger | $(8.98\pm0.57)*10^{24}$ | $(2.35\pm0.15)*10^{11}$ | $(2.09\pm0.22)*10^{13}$ |
| --- | --- | --- | --- | --- |
| R$^2$ | | 0.98 | 0.98 | 0.96 |

The activation energy and frequency factor obtained by the Kissinger and Ozawa methods are quite close, inducing confidence about the consistence of the obtained results. The parameter $E_a/RT$ has been calculated observing that only the first exothermic peak exceeds the upper limitation of 50, regarding the Kissinger method, and spanning between 55 and 56. The limitations of the parameter are possibly linked only with the accuracy of calculation, as explained by Flynn [25], without substantially affecting the theoretical validity of the model used. In other words, a limited exceeding of the limits of the parameter $E_a/RT$ is not expected to greatly affect the estimation of $E_a$ which, therefore, can be used and discussed. It is apparent that the first exothermic reaction evidenced by DSC involves a consistent amount of heat. A similar, although much smaller exothermic peak was evidenced and discussed by Garner's [30] and Block [20] (Figure 3). Interesting considerations are linked to this peak, which was associated to a surface reaction, initiating the subsequent primary decomposition. The hydrogen evolution associated with this reaction is small, approximately 1% of the theoretical total, as found by Garner. Considering the difficulty in obtaining and maintaining absolute purity of LiAlH$_4$, and also the magnitude of the heat effect, an impurity reaction of the type shown in Equation 1 is considered by Mikheeva et al. [31] the cause of the first exothermic peak. This is confirmed by examining samples deliberately exposed to the atmosphere, where the first exothermic peak increases with the exposure. The initial peak clearly appears to be associated with sample impurity. However, the reaction heat associated with the initial reaction proves to be an analytically useful means of assessing the purity of LAH samples or preparations.
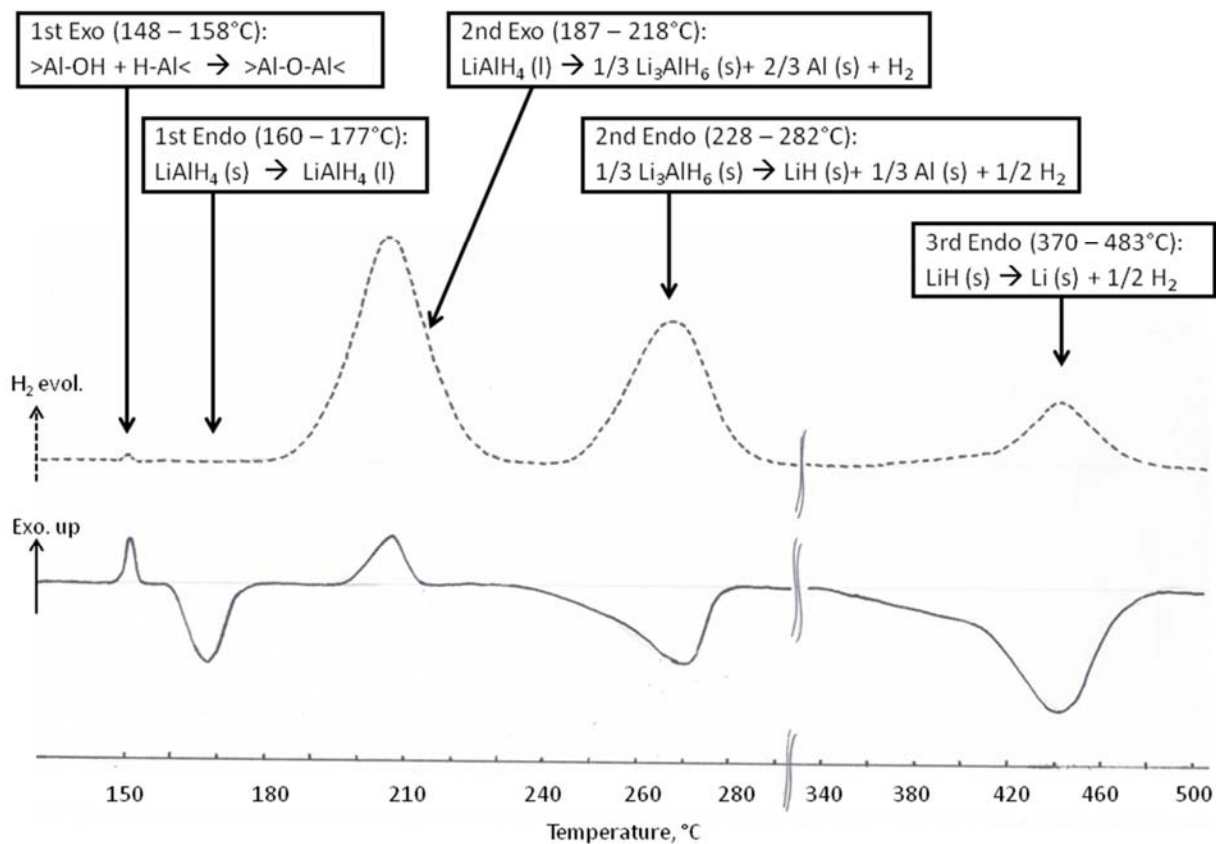
Figure 3: Schematization of a typical LAH decomposition process in which, both the DSC and H$_2$ evolution tests, are performed using Argon gas.

Observations carried out by Dymova and Andreasen seem to confirm this explanation. The last endothermic peak, corresponding to the lithium hydride decomposition, was outside the temperature range investigated in the present analysis. Considering the data obtained in the present work, especially taking into account the size of the first exothermic peak, a chemical interaction between the sample and the carrier gas (nitrogen) has been assumed, which will be discussed in the following sections. Argon gas was used by Block and Andreasen. Figure 4 shows two microphotographs of LAH, before (left) and after (right) a DSC test in nitrogen atmosphere. In order to protect LAH crystals from air moisture a mixture with a liquid dehydrated paraffin wax was carried out thus permitting to take some photos of good quality without sample decomposition. Pure LAH powder is a mixture of crystals with different shapes and dimensions while, after DSC test, the shape becomes similar to a (dark) sintered powder. LAH melting point is around 160 °C as stated by Andresen; this can explain why the dark powder is mainly composed by spherules

and not regular crystals. The reason why there were both a noticeable increasing in the sample mass occurring during a DSC test and the dark color of the residuals may be the occurrence of a chemical reaction between LAH and nitrogen (DSC heater gas) forming heavy dark nitride compounds.
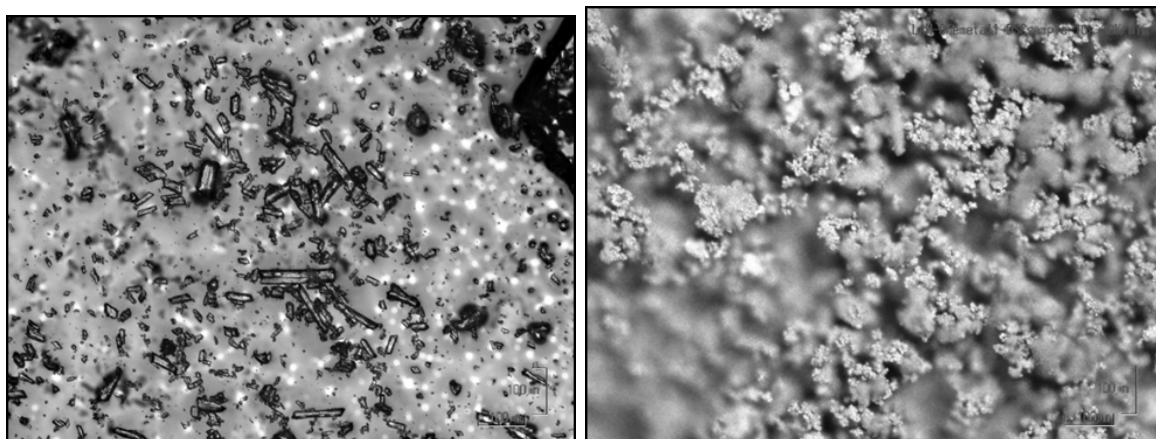


Figure 4. LAH crystals before (on the left) and after DSC test (on the right).

## IV.B.    Kinetic Calculations: L3AH

A markedly different behavior was observed with tri-lithium aluminum hexahydride. The DSC dehydrogenation curves for pure Li3AlH6 vs. the heating rate in nitrogen atmosphere are shown in Figure 5. There are two small exothermic peaks and two endothermic peaks.
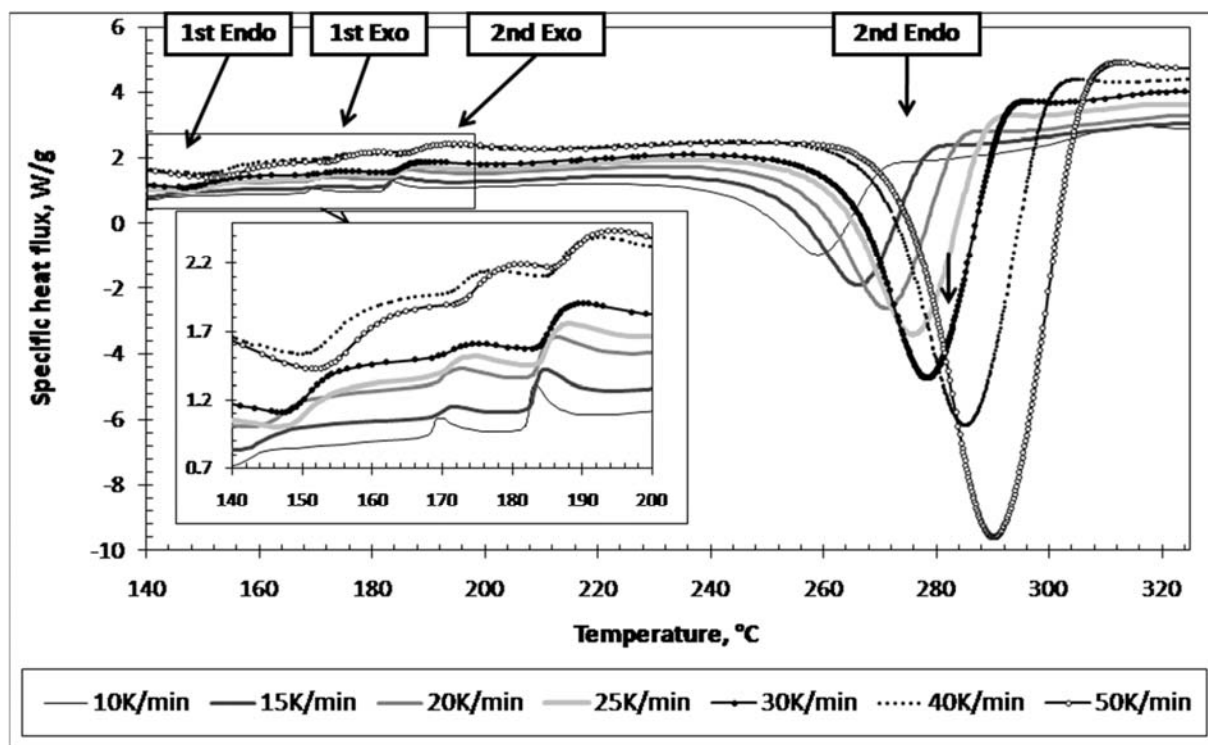
Figure 5. Kinetic DSC test: L3AH Chemetall.

Table 3 shows the list of the maximum peak temperature values, the initial and final sample mass and the percentage mass increase values. The values of the reaction heat linked with the first and second exothermic peak (third and fifth column respectively) and the first endothermic peak can be considered negligible when compared with the main endothermic peak (eighth column). As for the second endothermic peak, the values of the reaction heat are in the range 260 – 280 J/g for almost all values of thermal ramp.

**Table 3. List of temperature peak values with the corresponding initial and final sample mass for L3AH**

| β | 1st Exo | 1st Exo | 2st Exo | 2st Exo | 1st Endo | 2st Endo | 2nd Endo | $M_{in}$ | $M_{fin}$ | ΔM |
| | $T_p$ | Δh | $T_p$ | Δh | $T_p$ | $T_p$ | Δh | ± 0.1mg | ± 0.1mg | |
| [K/min] | [°C] | [J/g] | [°C] | [J/g] | [°C] | [°C] | [J/g] | [mg] | [mg] | [%] |
|---|---|---|---|---|---|---|---|---|---|---|
| 10 | 169.7 | 3.4 | 183.2 | 5.7 | 138.6 | 259.1 | 259 | 2.3 | 3.2 | 39.1 ± 10.4 |
| 15 | 171.7 | - | 184.9 | 4.4 | 140.1 | 266.2 | 280 | 2.3 | 3.2 | 39.1 ± 10.4 |
| 20 | 172.4 | 2.1 | 186.4 | 4.0 | 142.7 | 271.1 | 259 | 2.3 | 3.3 | 43.4 ± 10.6 |
| 25 | 172.4 | 1.5 | 188.4 | 3.3 | 146.7 | 275.9 | 262 | 2.3 | 3.0 | 30.4 ± 10.1 |
| 30 | 175.3 | - | 190.2 | 3.3 | 146.5 | 278.4 | 276 | 2.3 | 3.3 | 43.4 ± 10.6 |

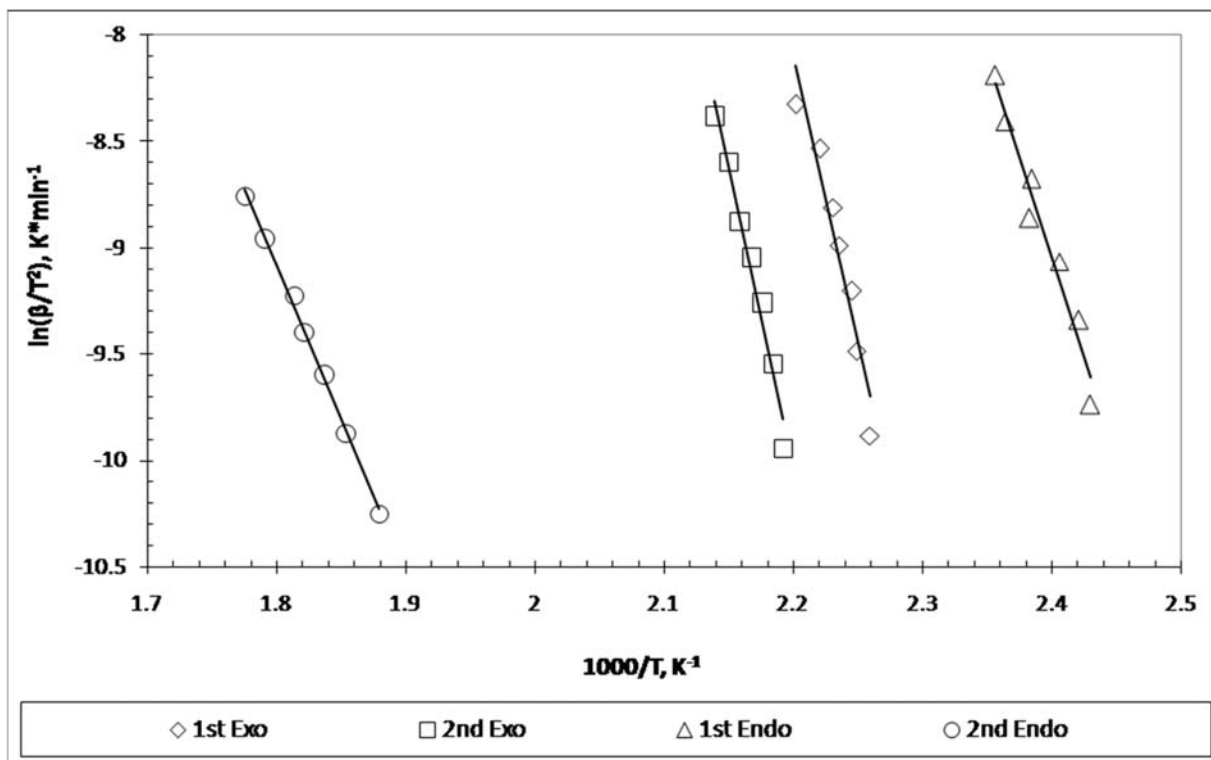| | | | | | | | | | |
|---|---|---|---|---|---|---|---|---|---|
| 40 | 177.4 | 1.1 | 192.2 | 3.0 | 150.1 | 285.2 | 274 | 2.2 | 3.1 | 40.9 ± 11.0 |
| 50 | 181.2 | - | 194.5 | 2.8 | 151.4 | 290.2 | 319 | 2.3 | 3.0 | 30.4 ± 10.1 |



Figure 6. Kinetic data processing (plotting -ln($\beta$ $T_p^2$) vs. 1/$T_p$ according to Kissinger's method): L3AH.

Figure 6 is obtained by plotting -ln($\beta$ $T_p^2$) vs. 1/$T_p$ according to Kissinger's method. Three barely noticeable peaks (first endothermic, first and second exothermic), probably associated to impurities decomposition process, were detected. Considering the corresponding temperature range (240 – 280 °C) of the last endothermic peak in LiAlH$_4$ dehydrogenation, the second endothermic peak was due to a decomposition process of Li$_3$AlH$_6$ (Equation 4), as shown in Figure 7. Table 4 shows E$_a$ and A values obtained using both Ozawa and Kissinger methods for all thermal events, calculating the slope and the intercept of the curve. The parameter E$_a$/RT has been calculated with the observation that both the first and second exothermic peaks exceed the upper limitation of 60 and 50, regarding respectively the Ozawa and Kissinger methods. Again, a small exceeding of the limits of the parameter should lead, at worst, to a less accurate estimation of E$_a$. Another consideration about the first two exothermic peaks must take into account their dimensions:

in contrast with the notable exothermic peaks of LAH, L3AH has shown slightly marked exothermic peaks. Again, the method of least squares and a 95% confidence interval were applied to estimate the uncertainty of the two most important kinetic parameters: $E_a$ and A.

**Table 4. Kinetic parameters for Li$_3$AlH$_6$, calculated by both Kissinger and Ozawa method**

| Kinetic Parameter | Method | 1$^{st}$ Exo (170 – 181°C) | 2$^{nd}$ Exo (183 – 194°C) | 1$^{st}$ Endo (139 – 151°C) | 2$^{nd}$ Endo (259 – 290°C) |
|---|---|---|---|---|---|
| $E_a$ [KJ/mol] | | 222.92±61.51 | 230.42±36.48 | 155.79±30.55 | 123.10±6.51 |
| A [min$^{-1}$] | Ozawa | $(3.36±0.17)*10^{26}$ | $(3.76±0.12)*10^{26}$ | $(7.48±0.28)*10^{19}$ | $(6.41±0.07)*10^{11}$ |
| $R^2$ | | 0.94 | 0.98 | 0.96 | 1.00 |
| $E_a$ [KJ/mol] | | 226.91±64.69 | 234.60±38.35 | 156.85±65.02 | 120.32±6.91 |
| A [min$^{-1}$] | Kissinger | $(1.00±0.05)*10^{27}$ | $(1.14±0.04)*10^{27}$ | $(1.02±0.04)*10^{20}$ | $(3.4±0.04)*10^{11}$ |
| $R^2$ | | 0.93 | 0.98 | 0.96 | 1.00 |

Activation energy and frequency factor obtained by the Kissinger and Ozawa methods are quite close, inducing confidence about the obtained experimental results. As it can be seen considering the values of confidence interval for activation energy, the uncertainty linked with all the small peaks (1$^{st}$ and 2$^{nd}$ exothermic and 1$^{st}$ endothermic peak) is higher than that linked with the 2$^{nd}$ endothermic peak: 61.51, 36.48, 30.55 KJ/mol Vs 6.51 KJ/mol. This could be mainly ascribed to two reasons: the presence of impurities and the link between L3AH and LAH. Starting from the last consideration, it is well known that one of the most used methods to obtain L3AH is through a controlled heat treatment on a mixture containing LiAlH4 and LiH. As well as every chemical reaction, small amounts of the reactants remain mixed with the reaction products. A sample of L3AH, therefore could also contain small amounts of LAH, LiH and other byproducts. The probable presence both of byproducts and traces of LAH, so, could explain not only the presence and the small size of the thermal peaks in the same thermal range in which LAH is thermally active, but also the dispersion of the experimental results. The second endothermic reaction occurring in L3AH at 259 - 290 °C is expected to produce the highest amount of hydrogen gas and is therefore the most interesting event.

# V. Discussion of Results
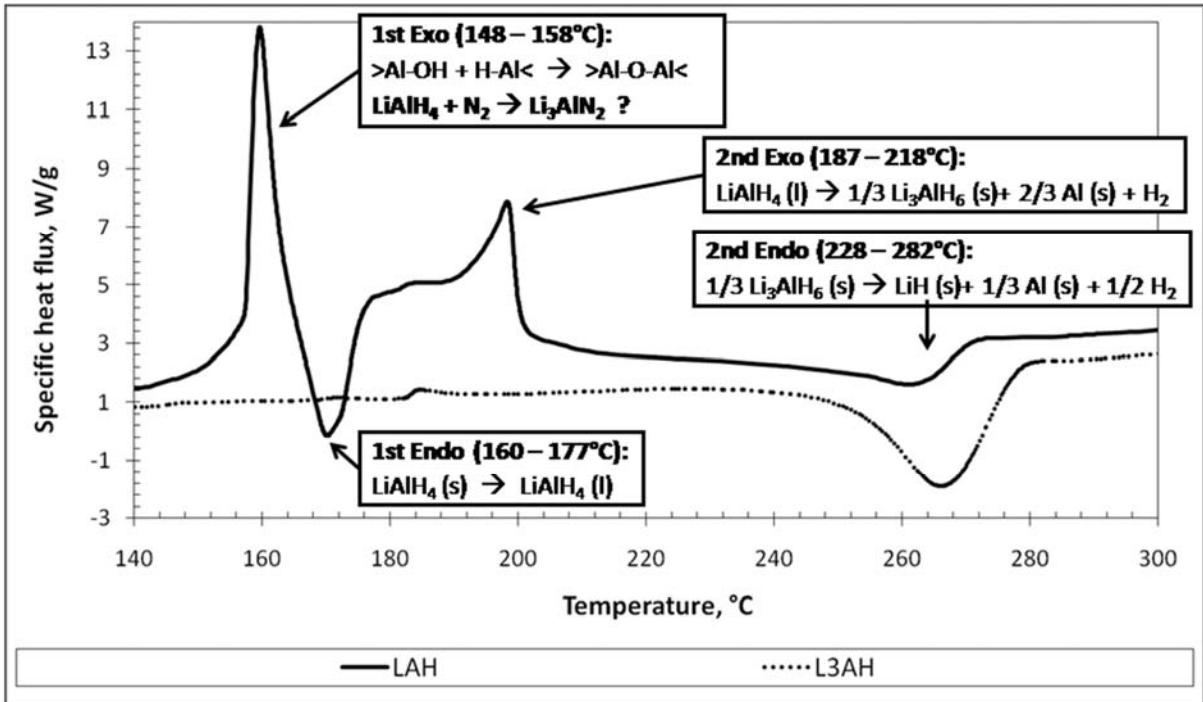
## V.A. Comparison between LAH and L3AH



Figure 7. Comparison between LAH and L3AH DSC tests performed at 15 K/min under nitrogen atmosphere.

In Figure 7 a comparison between the DSC curves of LAH and L3AH, at the same heating rate, is drawn to check the kinetic parameters. The only temperature range in which this is possible is 255 – 290 °C. The position of the main endothermic peak corresponds to the expected one at which theoretically LiH is formed. The area of the peak of LAH is smaller than that of L3AH because L3AH obtained by decomposition of the original LAH sample is mixed with metallic aluminum. A comparison between the values of heat of reaction calculated for the second endothermic peak of L3AH, (Table 3, column 8) and the values of $\Delta H$ (at the same value of $\beta$) (Table 1, column 7) for LAH, was drawn. The mean value of this ratio was $2.21 \pm 0.32$, which is close to the theoretical ratio, $2.12 \pm 0.08$ obtained by dividing the number of moles of the weighed amount of L3AH per one third of the number of moles of LAH (amount theoretically obtained after the thermal decomposition of LAH, Equation 3). The difference of 12.5% between the values of activation energy is small considering that there is no control upon the chemical reactions involved in the Li3AlH6 formation. The difference between activation energy data presented in the present work and those taken from literature (138.6 and 123.1 vs. 105 and 100 KJ/mol) could be due to the different TGA/DSC heater gas used and also to the sample preparation technique. By calculating the reaction rate at the same temperature (272 °C), the reaction rate values obtained (sixth column, Table 5) show a small difference which can be linked to the different values of both kinetic parameters. Higher activation energy is usually linked with a slower reaction rate because of the higher energy barrier of the reaction involved. The activation energy of LAH at 272 °C is higher than that of L3AH at the same temperature, thus indicating that a higher energy barrier has to be exceeded to have the decomposition reaction. Reactions of LAH lead to the formation of $Li_3AlH_6$ mixed with impurities (metallic aluminum, nitrides,..) which increase the energetic barrier responsible for dehydrogenation reaction. Pre-exponential factor values show an opposite behavior: $3.2*10^{13}$ min$^{-1}$ for LAH which is fifty times higher than that of L3AH. The described behavior of the kinetic parameter shows the reaction rate value for LAH to be close to that of L3AH.

**Table 5. Kinetic parameters for LAH and L3AH. (*) Data listed in the first column represent the temperature range of the maximum points of a selected peak (obtained at different heating rate values).**

| $T_p$ (*) | $E_a$ | $E_a$ (lit.) | A | k (272°C) |
|-----------|-------|--------------|---|-----------|
| [°C] | [KJ/mol] | [KJ/mol] | [min$^{-1}$] | [min$^{-1}$] |

| | | | | | |
|---|---|---|---|---|---|
| LiAlH$_4$ | 255 - 282 | 138.56±27.12 | 105 [*], 100 [**] | (3.17±0.34)*10$^{13}$ | 1.7 |
| | | 136.73±28.54 | | (2.09±0.22)*10$^{13}$ | |
| Li$_3$AlH$_6$ | 259 - 290 | 123.10±6.51 | - | (6.41±0.07)*10$^{11}$ | 1.0 |
| | | 120.32±6.91 | - | (3.40±0.04)*10$^{11}$ | |

Table 5 shows a comparison between the main endothermic peak of the LiAlH$_4$ and the main endothermic peak recorded in Li$_3$AlH$_6$ thermographs. It can be observed that the temperature range in which the endothermic peak points fall is the same for both metal hydrides. Moreover, there is good agreement between all the obtained kinetic data; in particular, the rate constant k(T) (calculated at 272 °C) is very close for both substances. The difference between the values of the rate constant (1.7 and 1.0 respectively) can be considered small considering the high sensitivity of the Arrhenius's law with the pre-exponential factor. The limited difference in terms of activation energy could be due to the LAH decomposition process (Equation 3), in which metallic aluminum is formed as byproduct (lacking in L3AH sample). The thermal contribution during the following L3AH decomposition (Equation 4) is not negligible.

**V.B.    Sample Mass Increase: Proposed Explanation**

The increase of the sample weight observed at the end of DSC tests is due to a reaction with nitrogen. The probability to obtain this chemical reaction at low temperatures (close to first exothermic peak in the range 160 –169 °C) is usually low because of the very low chemical reactivity of nitrogen. At higher temperatures and in presence of lithium-aluminum alloys, chemical nitridation reactions could occur [33-34]. Therefore, it is reasonable to believe that the thermal behavior of LAH is strictly linked to the purity of the sample, to the presence of moisture and to reactivity of the DSC carrier gas. In the literature very few results concerning the reaction between nitrogen gas and LAH can be found. Simone and Bruno [15], studying lithium hydride as solid fuel for scramjet propulsion, observed that the reaction between Li and dried N$_2$ is 10 to 15 times more rapid than in air. In particular, liquid lithium will not react with dry oxygen, but in presence of only 15 ppm of moisture, the reaction rate strongly increases, thus allowing the reaction with air, nitrogen, oxygen and also carbon dioxide. Gardner [35] proposed a model of gas-liquid reaction for the explanation of the reaction between nitrogen and molten lithium which involves three phenomena. The first one is the chemisorption of nitrogen followed by the conversion of N$_2$ to Li$_3$N and finally the dissolving of lithium nitride

---

* Andreasen, TGA tests performed using argon as heating gas.
** McCarty [32], TGA tests performed using helium as heating gas, all the LAH samples have been re-crystallized, purified and filtered.

in the molten lithium. As the liquid lithium is saturated by $Li_3N$, a layer of nitride is formed on the surface and the reaction rate is controlled by mass transport of $N_2$ through the surface layer of nitride. Besson [36] and Jeppson [37] studied the influence of moisture on the lithium/nitrogen reaction, showing that a moisture content of 10 ppm increases the rate of reaction between Li and $N_2$. Another result was linked with the need to have a LiOH layer on the lithium surface to explain the tendency of Li to react with nitrogen, giving $Li_3N$ at low temperatures. A TGA test performed by Markowitz [38] showed the reaction between lithium and nitrogen and, in particular, the differences between dry and moist nitrogen. Considering the reaction involving dry nitrogen, before the melting point of the metal lithium (close to 170 °C), the reaction is apparently negligible. Considering the reaction between Li and nitrogen containing moist, the reaction starts at room temperature, but above the melting temperature the reaction proceeds as fast as the reaction with dry nitrogen. Observing the fast reaction shown by TGA thermograph, Markowitz suggested that the ignition temperature of lithium in nitrogen occurs at 170 °C. This is also supported by the DSC tests carried out and shown in Figure 1, and in particular with the temperature of the first exothermic peak which falls at a temperature value close to 170 °C, depending on the chosen heating ramp. Frankenburger [39] studying the chemical reaction between nitrogen and lithium observed that the reaction rate is dependent on the rate of diffusion of nitrogen through the layer of $Li_3N$ and this was confirmed by Rhein [16], who proposed a simplified model of combustion of lithium under nitrogen flow. Barnett [40], by burning lithium with a nitrogen flow, collected a deposit of a black ceramic layer of Li3N, on the bottom of the reactor used for the experimental tests. Data shown in Table 6 and Figure 8, have been obtained using a DSC apparatus in which the thermal range 30°C-350°C was divided into four stages corresponding to the LAH main exothermic and endothermic peaks. Four samples, both for LAH and L3AH, were weighed before and after the chosen thermal stage thus obtaining information about the mass increase. Only for this experiment, a higher mass (10 mg instead of 2 mg) of the sample was selected to achieve a higher accuracy on the estimation of the mass increase. In order to evaluate the influence of the heating rate on the sample mass increase, four experiments were performed at 10 K/min and one at 2.5 K/min. Figure 8 shows all the traces investigated. For LAH the main mass increase is observed at the end of the first endothermic peak at 182 °C (Fig. 8, dashed grey line, %ΔM) with a mass increase of 21%. In the range 182 -220 °C, between the first endothermic peak and the second exothermic peak, the reaction reaches almost the maximum of the percentage mass increase of about 32.8%. At the temperature of 350 °C, corresponding to the end of the second endothermic peak, the percentage mass increase value is 33.1% indicating that between 220 and 350 °C the reaction is over. As for the peaks of 10 mg samples (10-10-180, 10-10-220 and 10-2.5-350), they are smaller than exothermic and endothermic peaks for 2 mg samples. A thermograph obtained at 2.5 K/min

is added to the plot in order to show how complex the reaction involved in the narrow temperature range of 140 - 220 °C is. The presence of an endothermic peak immediately after an exothermic peak is well known in the study of explosives decomposition kinetics [41 - 43]. The behavior of L3AH, shown in Table 6, appears different due to higher mass increase (from 11% to 40%) at the main endothermic peak in the temperature range 220 - 280 °C at 10 K/min. The measured heat of reaction listed in Table 3 shows the difference among the peaks occurring before 220 °C and the main endothermic peak (3-6 J/g versus 260 J/g) at 259 °C. The observed behavior is affected by the ratio between the sample mass and the surface area exposed to nitrogen gas and by a complex reaction occurring in the thermal range 140 - 180 °C. A sample mass of about 2 mg is a good trade-off between the need to perform DSC tests at high heating rate values (higher than 10 K/min) and to grant good accuracy of the thermograph. The amount of powder is weighed and homogeneously distributed inside the aluminum pan (6.5 mm diameter) to obtain a layer with a regular depth in order to have reproducible results. By weighing a sample mass five times higher, the depth of the powder layer inside the DSC pan is higher and nitrogen cannot reach each crystal of the sample. As a consequence, considering the DSC thermographs in Figure 5-b, those obtained by weighing a mass of 10 mg sample (LAH_30-160, LAH_30-180 and LAH_30-220) show exo and endo peaks different both in shape and dimensions with respect to that obtained with the 2 mg mass sample (LAH_30-350).

**Table 6.  Sample mass increase obtained using a DSC apparatus**

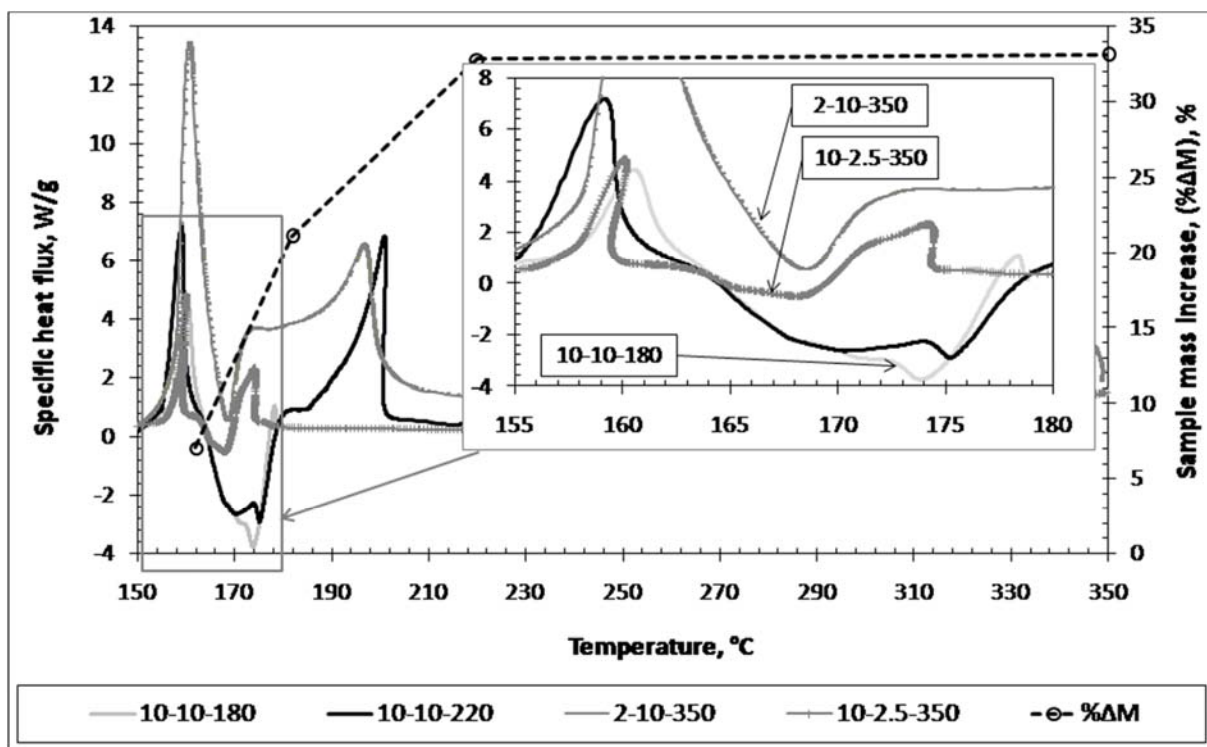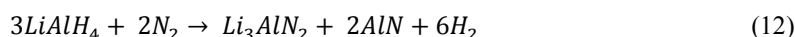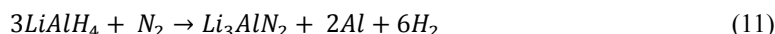|  | 1st Exo 30-162°C $\Delta M$ [%] | 1st Endo 30-182°C $\Delta M$ [%] | 2nd Exo 30-220°C $\Delta M$ [%] | 2nd Endo 30-350°C $\Delta M$ [%] |
|---|---|---|---|---|
| LAH | 7.1 ± 7 | 21.1 ± 9 | 32.8 ± 3 | 33.1 ± 7 |
| L3AH | - | 8.3 ± 8 | 11.1 ± 6 | 40.0 ± 8 |

Figure 8. Percentage mass increase of LAH samples, compared with DSC tests obtained for different thermal ranges matching the main exo and endothermic peaks. The legend shows three numbers: the sample mass, the heating rate and the maximum temperature reached (e.g. 10-2.5-350 means 10 mg, 2.5 K/min, $T_{max}$ 350°C).

The sample mass increase observed for all the DSC test performed in the present work (Table 1 and Table 3) can be explained with the following reaction schemes:

$$3LiAlH_4 + N_2 \rightarrow Li_3AlN_2 + 2Al + 6H_2 \qquad (11)$$

$$3LiAlH_4 + 2N_2 \rightarrow Li_3AlN_2 + 2AlN + 6H_2 \qquad (12)$$

Referring to reaction 11, an increase in sample mass of 14.0 % is expected; in reaction12, the expected theoretical percentage sample mass increase is 38.6 %. Considering trilithium aluminum hydride (reaction 13), an increase of the sample mass expected is about 40.8%.

$$Li_3AlH_6 + N_2 \rightarrow Li_3AlN_2 + 3H_2 \qquad (13)$$
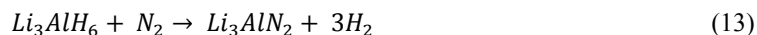
The average increase of weight of LAH samples for temperature ramp higher than 10 K/min, is 26.1 ± 9.9 % (Table 1), which means a value between 16.2% and 36.0%. At the lowest temperature ramp, the increase of sample weight is higher, ranging between 21.2% and 42.4%. A higher average value can be observed for L3AH samples in the range 38.1 ± 10.5 % (Table 3), which means a value between 27.6% and 48.6%.

## VI. Conclusions

In this paper the effect of nitrogen, used as heating gas in DSC apparatus, on kinetic parameters and thermal behavior of lithium aluminum hydride ($LiAlH_4$) and tri-lithium aluminum hydride ($Li_3AlH_6$) is investigated. Exothermic peak in the thermal range 162 - 170 °C obtained using nitrogen is different from the one obtained using argon or helium. A nitridation reaction can explain the increase of the sample mass after each DSC test (26 ± 9.9% for LAH and 38 ± 10.5% for L3AH). It does match the obtained experimental data. The main increase of LAH sample mass usually occurs in the thermal range 160 - 180°C, increasing from 7.1% to 21.1%. For L3AH, the mass increase is concentrated in the thermal range 220 - 350 °C, increasing from 11.1% to 40%. Ozawa and Kissinger methods, giving kinetic parameters (activation energy $E_a$ and frequency factor A) are used. A comparison between two DSC traces, one of LAH and one of L3AH at the same heating rate, shows that the last endothermic peak, occurring in the thermal range 255 - 290 °C, reaches a minimum roughly at the same temperature (261 - 266 °C at 15 K/min). This points out that during the thermal decomposition of LAH a small fraction of L3AH is formed. The calculated values of activation energy for LAH and L3AH at 272 °C are 138.56±27.12 and 123.10±6.51 KJ/mol respectively. By calculating the reaction rate at 272 °C, both for LAH and L3AH, the results indicate a small difference 1.7 and 1.0 $min^{-1}$ respectively due to the compensating effect of the pre-exponential factor. On the basis of DSC thermographs of LAH and the curve describing the sample mass increase with temperature, it can be inferred that a set of chemical reactions occurs between the first exothermic peak (140 - 180 °C) and the second exothermic peak (180 – 220 °C). As a consequence, a strict application of both Ozawa's and Kissinger's methods may not be appropriate. The reaction of lithium aluminum hydrides with nitrogen gas has confirmed important trends of the couple metallic lithium/nitrogen. Thanks to the high hydrogen content, the materials tested could be suitable for airbreathing propulsion applications. The high reactivity with moisture, even with the metallic lithium, extensively studied in the past, could be overcome by using special hydrophobic additives.

## References

[1]     Osmon, R. V., "An Experimental Investigation of Lithium Aluminum Hydride-Hydrogen Peroxide Hybrid Rocket", Aerospace Chemical Engineering, Vol. 62, 1966, pp. 92-102.

[2]     Humble, R. W.,"Fuel performance enhancements for hybrid propulsion", AIAA paper 2000-3437, 2000. Doi: 10.2514/6.2000-3437.

[3]     Il'in, A.P., Bychin, N.V., and Gromov, A.A., "Products of combustion of aluminum hydride", Combustion Explosion and Shock Waves, Vol. 37, 2001, pp. 490-491.

[4]     Calabro, M., "LOX/HTPB/AlH3 hybrid propulsion for launch vehicle boosters", AIAA Paper 2004-3823, 2004. Doi: 10.2514/6.2004-3823.

[5]     Corpening, J.H., Palmer, R.K., and Heister, S.D., "Combustion of advanced non-toxic hybrid propellants", International Journal of Alternative Propulsion, Vol. 1, 2007, pp. 154-173. Doi: 10.1504/IJAP.2007.013018.

[6]     DeSain, J.D., Curtiss, T.J., Cohen, R.B., and Brady, B.B., "Testing of $LiAlH_4$ as a potential additive paraffin wax hybrid rocket fuel", Physical Sciences Laboratories, Report No. TR-2008(8506)-1, El Segundo, CA, USA, 2008.

[7]     Boyce, R.R., Tirtei, S.C., Brown, L., Creagh, M., and Ogawa, H., "SCRAMSPACE: scramjet-based access-to-space systems", AIAA Paper 2011-2297, 2011. Doi: 10.2514/6.2011-2297.

[8]     Smart, M.K., and Tetlow, M.R., "Orbital delivery of small payloads using hypersonic airbreathing propulsion", Journal of Spacecraft and Rockets, Vol. 46, No. 1, 2009, pp. 117-125. Doi: 10.2514/1.38784.

[9]   Mitani, T., and Kouchi, T., "Flame structures and combustion efficiency computed for a Mach 6 scramjet engine", Combustion and Flame, Vol. 142, 2005, pp 187-196. Doi: 10.1016/j.combustflame.2004.10.004.

[10]    Potturi, A.S., and Edwards, J.R., "Large-eddy/Reynolds-averaged navier-stokes simulation of cavity-stabilized ethylene combustion", *Combustion and Flame*, Vol. 162, 2015, pp. 1176-1192. Doi: 10.1016/j.combustflame.2014.10.011.

[11]    Dimotakis, P., "100 lbf to low earth orbit (LEO): small-payload launch options", Defense Advanced Research Projects Agency, Report No. JSR-98-140, McLean, VA, USA, 2000.

[12]    Witt, M.A., "Investigation into the feasibility of using solid fuel ramjets for high supersonic/low hypersonic tactical missiles", Ph.D. Dissertation, Dept. of Aeronautics and Astronautics, Naval Postgraduate School, Monterey, CA, 1989.

[13]    Angus, W.J., "An investigation into the performance characteristics of a solid fuel scramjet propulsion device", Ph.D. Dissertation, Dept. of Aeronautics and Astronautics, Naval Postgraduate School, Monterey, CA, 1991.

[14]    Cohen, A., and Natan, B., "Experimental investigation of a supersonic combustion solid fuel ramjet", Journal of Propulsion and Power, Vol. 14, No. 6, 1998, pp. 880-889. Doi: 10.2514/2.5379.

[15]    Simone, D., and Bruno, C., "Preliminary investigation on lithium hydride as fuel for solid-fueled scramjet engines", Journal of Propulsion and Power, Vol. 25, 2009, pp. 875-884. Doi: 10.2514/1.39136.

[16]  Rhein, R.A., "Lithium combustion: a review", Naval Weapons Center, Report No. NWC TP 7087, China Lake, CA, USA, 1991.

[17]  Dymova, T.N., Aleksandrov, D.P., Konoplev, V.N., Silina, T.A., and Sizareva, A.S., Russian Journal of Coordination Chemistry, Vol. 20, 1994, pp. 279-285.

[18]  Andreasen, A., "Effects of Ti-doping on the dehydrogenation kinetic parameters of lithium aluminum hydride", Journal of Alloys and Compounds, Vol. 419, 2006, pp. 40-44. Doi: 10.1016/j.jallcom.2005.09.067.

[19]  Ismail, M., Zhao, Y., Yu, X.B., and Dou, S.X., "Effects of $NbF_5$ addition on the hydrogen storage properties of $LiAlH_4$", International Journal of Hydrogen Energy, Vol. 35, 2010, pp. 2361-2367. Doi: 10.1016/j.ijhydene.2009.12.178 .

[20]  Block, J., and Gray, P., "The thermal decomposition of lithium aluminum hydride", Inorganic Chemistry, Vol. 4, 1965, pp. 304-305.

[21]  Balema, V.P., Pecharsky, V.K., and Dennis, K.W., "Solid state phase transformations in $LiAlH_4$ during high-energy ball-milling", Journal of Alloys and Compounds, Vol. 313, 2000, pp. 69-74. Doi: 10.1016/S0925-8388(00)01201-9.

[22]  Wang, J., Laborie, M.P.G., and Wolcott, M.P., "Comparison of model-free kinetic methods for modeling the cure kinetics of commercial phenol-formaldehyde resins", Thermochimica Acta, Vol. 439, 2005, pp. 68-73. Doi: 10.1016/j.tca.2005.09.001.

[23]  Friedman, H.L., "Kinetics of thermal degradation of char-forming plastics from thermogravimetry. Application to phenolic plastic", Journal of Polymer Science, Part C, Vol. 6, 1964, pp. 183-195. Doi: 10.1002/polc.5070060121.

[24]  Kissinger, H.E., "Variation of peak temperature with heating rate in differential thermal analysis", Journal of Research of the National Bureau of Standards, Vol. 57, 1956, pp. 217-221.

[25]  Flynn, J.H., and Wall, L.A., General treatment of thermogravimetry of polymers, Journal of Research of the National Bureau of Standards-A. Physics and Chemistry, Vol. 70A, 1966, pp. 487-523, Doi: dx.doi.org/10.6028/jres.070A.043.

[26]  Doyle, C.D., "Kinetic analysis of thermogravimetric data", Journal of Applied Polymer Science, Vol. 5, 1961, pp. 285-292. Doi: 10.1002/app.1961.070051506.

[27] Sbirrazzuoli, N., Girault, Y., and Elegant, L., "Simulations for evaluation of kinetic methods in differential scanning calorimetry. Part 3 – Peak maximum evolution methods and isoconversional methods", Thermochimica Acta, Vol. 293, 1997, pp. 25-37. Doi: 10.1016/j.ijhydene.2009.12.178.

[28] Sbirrazzuoli, N., Vincent, L., Mija, A., and Guigo, N., "Integral, differential and advanced isoconversional methods: complex mechanisms and isothermal predicted conversion-time curves", Chemiometrics and Intelligent Laboratory Systems, Vol. 96, 2009, pp. 219-226. Doi: 10.1016/j.chemolab.2009.02.002.

[29] Farjas, J., and Roura, P., "Isoconversional analysis of solid state transformations", Journal of Thermal Analysis and Calorimetry, Vol. 105, 2011, pp. 757-766. Doi: 10.1007/s10973-011-1446-4.

[30] Garner, W.E., and Haycock, E.W., Proceedings of the Royal Society of London, Vol. A211, 1952.

[31] Mikheeva, V.I., Selivokhina, M.L., and Kryukova, O.N., Proceedings of the USSR Academy of Science-Chemical Section, Vol. 109, 1956, pp. 439.

[32] McCarty, M. Jr., Maycock, J.N., and. Pai Verneker V.R., "Thermal decomposition of LiAlH$_4$", Journal of Physical Chemistry, Vol. 72, 1968, pp. 4009-4014. Doi: 10.1021/j100858a012.

[33] Bogdanovic, B., Studiengesellschaft, Kohle Mbh (Mulheim an der Ruhr, DE), "Alkali metal complex compounds, and their use in the hydrogenation and nitridation of alkali metals", US Patent, 4396589, filed 29 Sept. 1983.

[34] Selvaduray, G., and Sheet, L., "Aluminum nitride: review of synthesis methods", Materials. Science and Technology, Vol. 9, 1993, pp. 463-473. Doi: 10.1179/mst.1993.9.6.463.

[35] Gardner, M.P., and Altermatt, R.E., "Kinetics of the reaction of hydrogen and nitrogen with molten lithium, Lithium: Current Applications in Science, Medicine and Technology, R.O. Bach, Wiley, New York, N. Y, 1985, pp. 195-206.

[36] Besson, J., and Muller, W., "The reaction of nitrogen on lithium at ordinary temperatures and the role of water vapor in this reaction", Compt. Rend., Vol. 247, 1958, pp. 2370-2372.

[37] Jeppson, D.W., "Lithium literature review: lithium's properties and interactions". Hanford Engineering Development Laboratory, Report HEDL-TME 78-15, UC-20, Richland, WA., USA, 1978.

[38] Markowitz, M.M., and Boryta, D.A., "Lithium metal-gas reactions, interaction of lithium metal with air and its component Gases", Journal of Chemical and Engineering Data, Vol. 7, 1962, pp. 586-591. Doi: 10.1021/je60015a047.

[39]  Frankenburger, W., "The chemical union of nitrogen to lithium and the mechanism of this reaction", Z. Elektrochem., Vol. 32, 1926, pp. 481-491.

[40]  Barnett, D.S., Gil, T.K., and Kazimi, M.S., "Lithium-mixed gas reactions", Plasma Fusion Center and the Department of Nuclear Engineering, Report PFC/RR-89-3, Massachusetts Institute of Technology, Cambridge, MA, 1989.

[41]  Da Silva, G., Iha, K., Cardoso, A.M., Mattos, E.C., and Dutra, R.C.L., "Study of the thermal decomposition of 2,2',4,4',6,6'- hexanitrostilbene", Journal of Aerospace Technology and Management, Vol. 2, 2010, pp. 41-46. Doi: 10.5028/jatm.v2i1.39.

[42]  Lee, J.S., Hsu, C.K., and Chang, C.L., "A study on the thermal decomposition behaviors of PETN, RDX, HNS and HMX", Thermochimica Acta, Vol. 392, 2002, pp. 173-176. Doi: 10.1016/S0040-6031(02)00099-0.

[43]  Long, G.T., Vyazovkin, S., Brems, B.A., and Wight, C.A., "Competitive vaporization and decomposition of liquid RDX", The Journal of Physical Chemistry B, Vol. 104, 2000, pp. 2570-2574. Doi: 10.1021/jp993334n.